Colloidal systems with a short-range attraction and long-range repulsion: Phase diagrams, structures, and dynamics

Yun Liu[1,2,3] and Yuyin Xi[1,2]

Abstract

Colloidal systems with both a short-range attraction and long-range repulsion (SALR) have rich phases compared with the traditional hard sphere systems or sticky hard sphere systems. The competition between the short-range attraction and long-range repulsion results in the frustrated phase separation, which leads to the formation of intermediate range order (IRO) structures and introduces new phases to both equilibrium and nonequilibrium phase diagrams, such as clustered fluid, cluster percolated fluid, Wigner glass, and cluster glass. One hallmark feature of many SALR systems is the appearance of the IRO peak in the interparticle structure factor, which is associated with different types of IRO structures. The relationship between the IRO peak and the clustered fluid state has been careful investigated. Not surprisingly, the morphology of clusters in solutions can be affected and controlled by the SALR potential. And the effect of the SALR potential on the dynamic properties is also reviewed here. Even though much progress has been made in understanding SALR systems, many future works are still needed to have quantitative comparisons between experiments and simulations/theories and understand the differences from different experimental systems. Owing to the large parameter space available for SALR systems, many exciting features of SALR systems are not fully explored yet. Because proteins in low-salinity solutions have SALR interactions, the understanding of SALR systems can greatly help understand protein behavior in concentrated solutions or crowded conditions.

Addresses

[1] Center for Neutron Research, National Institute of Standards and Technology, Gaithersburg, MD, 20899, USA
[2] Department of Chemical & Biomolecular Engineering, University of Delaware, Newark, DE, 19716, USA
[3] Department of Physics & Astronomy, University of Delaware, Newark, DE, 19716, USA

Corresponding author: Liu, Yun (yunliu@nist.gov), (yunliu@udel.edu)

Introduction

Colloids are commonly encountered in many materials of our daily life. They can exist in a wide range of shapes and compositions, such as micelles, quantum dots, proteins, star polymers, synthetic nanoparticles, and active colloids. Studying the structure and dynamics of colloidal systems is essential to understand, control, and predict the macroscopic properties of these materials [1−4]. Model colloidal systems have been serving as important testbeds to prove theories and demonstrate the underlining physics mechanisms of many interesting phenomena in complicated systems [3,5−7]. Commonly studied model systems are usually spherical particles with isotropic interactions. Even though this is, to some extent, an oversimplification of most real systems, information obtained from these model systems has been shown to be tremendously useful for us to understand complex interactions between many soft-matter materials [1,8−10]. Spherical systems with hard sphere (HS) interactions are arguably the most well-studied class of colloidal systems [5]. And HS systems with a short-range attraction, or sticky HS (SHS) systems, have also been extensively studied in the past several decades [2,4,6]. More recently, the colloidal science community has seen the increased interests in studying HS systems with both a short-range attraction and long-range repulsion (SALR) [10−17].

SALR interaction is not something new to the colloidal science community. Many charged colloidal particles have been demonstrated to have SALR interactions. At certain conditions, the well-known Derjaguin−Landau−Verwey−Overbeek potential is one type of SALR interactions [8]. For many proteins in low-salinity solutions, it has been long recognized that there should be both a short-range attraction and long-range repulsion between them [18−21]. Because the attraction favors the formation of aggregates that can eventually lead to the phase separation of a system, it has been a widely used practice by introducing charge repulsions to stabilize a colloidal system [8]. The revived interests in

the past decade for colloidal systems with SALR interactions have been triggered by understanding the structures and dynamics of SALR systems in solutions when the range of the repulsion is relatively long. Especially, there have been strong interests in the cluster formation in the liquid states and their consequence to the macroscopic properties of the solutions [12,13,16,17,22–24]. It is important to point out that protein cluster formation has been found also important to control the viscosity of many therapeutic proteins [1,25–28]. Hence, there is a strong interest from the industry to understand the reversible self-association, or clusters, in concentrated proteins solutions [25,28]. Even though many therapeutic proteins, such as monoclonal antibodies, have irregular shapes with anisotropic potentials, the properties of some protein solutions can be qualitatively explained by a SALR interaction [25,29]. Also, by controlling the parameters of the SALR interaction, particles in solutions can self-assemble into interesting structures, which can potentially lead to a new way to synthesize materials [30,31]. And the competitive nature of the short-range attraction and long-range repulsion also has profound impact on the gelation and glass transitions of SALR systems compared with the widely studied SHS systems [14–17,32,33].

A typical SALR interaction potential, $V(r)$, can be expressed as

$$\beta V(r) = \beta V_{SA}(r) + \beta A \frac{e^{-Z(r-1)}}{r}$$

where $\beta = \frac{1}{k_B T}$ and k_B is the Boltzmann constant and T is the absolute temperature. r is the center-to-center distance between two particles normalized by the particle diameter, σ. $V(r)$ is an effective potential based on the mean field concept by including the effects of all solvent molecules, such as counterions, coions, and any other small solvent molecules added to the solution. $V_{SA}(r)$ represents a short-range attraction. And the second term is a Yukawa function that has been commonly used in many works to represent the long-range repulsion. This is not surprising as in most experimental SALR systems, the long-range repulsion is due to the screened Coulombic repulsion. Thus, A is the strength of the repulsion that always has a positive value. And $1/Z$ can be considered the range of the repulsion normalized by σ. Unlike the function form of the long-range repulsion, $V_{SA}(r)$ has many different forms in literature. The commonly used functions for $V_{SA}(r)$ includes Yukawa function, Lennard-Jones potential, and square well [12,15,34–36]. The physical origins of the short-range attraction can be different for different experimental systems, such as due to depletion attraction [6,16,17,37], bridging attraction [38,39], counterion-mediated attraction [40], or hydrophobic–hydrophilic surfaces [41]. The equilibrium solution structure and phase diagrams are expected to be similar as long as the effective interaction is identical [13,42,43]. However, the

nonequilibrium phase diagrams and dynamics of systems can be different for systems with identical effective interactions but with different physics origins [39,44].

Because there are two control parameters (range and strength) for either attraction or repulsion, there are at least total four control parameters for a system with an SALR interaction. Based on the potential parameters that have been explored in literature, most SALR systems studied recently can be approximately categorized into three different types of SALR systems. For the type I, the range of $V_{SA}(r)$ is less than 20% of the particle diameter, and the range of repulsion is only a fraction of the particle diameters. Hence, Z is usually larger than 1. For the type II, the range of $V_{SA}(r)$ is still less than 20% of the particle diameter, but the range of repulsion is comparable or larger than the particle diameter. Hence, Z is usually less than 1. For the type III, the range of $V_{SA}(r)$ is significantly larger than 20% of the particle diameter but still smaller than the range of the repulsion. Table 1 shows the potential parameters of a selected list of SALR systems. The difference of parameters used in different types of SALR systems has strong impacts on the structures and dynamics of SALR systems. The type-I systems are most commonly encountered in experimental SALR systems [12,14,16,45]. Computer simulation and theoretical works cover the cases for both the type-I and type-II systems [13,15,23,36]. There are relatively small number of works on the type-III systems [46,47]. Note that the aforementioned classification is only an empirical approach based on the parameters used in different studies.

In this article, we would like to review the recent progress of studying SALR systems by focusing on the phase diagrams, structures, and dynamics. The physical origins of effective interactions of different experimental systems may be mentioned but will not be discussed in this article due to limited space. We will mainly focus on the progress for the type-I and type-II SALR systems but will also briefly discuss the type-III systems. There may be other types of SALR systems that do not belong to the three types of systems mentioned here and will not be discussed in this article. Even though we tried to include many relevant works, we are certainly biased by our own research experience and thus may have unintentionally omitted some important works. In addition, the limited space here does not allow us to have an exhaustive review of all works.

Phase diagrams of SALR systems

For systems without long-range repulsions, attractions can drive the phase separation. When introducing an additional long-range repulsion, the phase separation can be suppressed, resulting in a frustrated phase separation or microphase separation [13,15,23,

Table 1

The parameters of the SALR interactions are listed for a selected list of references, in which the potential parameters are given or can be estimated.

Method	Ref	Year	First author	Range of SA	Z	Type	Diameter	Particles
Experiment	[16]	2005	Campbell	0.13	1.55	I[a]	1.55 um	PMMA
Experiment	[35]	2007	Cardinaux	≈ 0.036	1 to 3.4	I	~3.4 nm	Lysozyme
Experiment	[48]	2008	Shukla	<0.1	1.1 to 3.3	I	~3.4 nm	Lysozyme
Experiment	[17]	2010	Klix	0.19	≈ 1	I and II[a]	1.95 um	PMMA
Experiment	[12]	2011	Liu	0.1	2 to 4	I	~3.4 nm	Lysozyme
Experiment	[45]	2012	Zhang	0.028	0.56	II[a]	0.892 um	PMMA
Experiment	[14]	2015	Godfrin	0.1	1.2 to 4.4	I	~3.4 nm	Lysozyme
Simulation	[15]	2004	Sciortino	0.03	0.5	II		
Simulation	[49]	2008	Toledano	0.03	0.5	II		
Simulation	[36]	2013	Valadez	0.01	1.6	I		
Simulation	[13]	2015	Godfrin	<0.2	0.5, 2[b]	I and II		
Simulation	[23]	2015	Jadrich	≈ 0.03	0.5	II		
Simulation	[50]	2016	Bollinger	≈ 0.1	0.25−1.4	I and II		
Simulation	[51]	2016	Ioannidou	≈ 0.2	2	I and II		
Simulation	[52]	2018	Das	<0.05	0.56	II		
Theory	[53]	2004	Mossa	0.03	0.5, 0.8, 2	I and II		
Theory	[54]	2004	Wu	0.1	0.5	II		
Theory	[46]	2007	Archer	1	0.5	III		
Theory	[55]	2008	Archer	1	0.5	III		
Theory	[56]	2015	Riest	0.1	0.5	II		

SALR, short-range attraction and long-range repulsion; PMMA, Poly(methyl methacrylate).

This is not a complete list of all references in this article. Based on the range of the SA and the range of repulsion $(1/Z)$, these works are empirically classified into three types of SALR systems. The details are given in the main text. The particle materials together with their diameters are also listed for experimental articles.

[a] The interaction potential for most PMMA systems is estimated at relatively low concentrations. The potential parameters may change at higher concentrations.

[b] In this article, most discussions have been focused on $Z = 0.5$.

47,50,57]. This frustrated phase separation results in an intermediate range order (IRO) that will be discussed in detail later in this article [12,13]. For HS systems or charge repulsion systems, particles tend to disperse relatively uniformly at a long-range length scale. For SHS systems, the attraction drives the particle aggregation to form heterogeneous density distribution at the large length scale that form fractal clusters spanning through the whole system [4]. SALR systems have the features of both HS and SHS systems. At the length scale smaller than that of the IRO, the attraction drives the formation of heterogeneous density distribution [14,32]. But the repulsion can stop the growth of the heterogeneous clusters and result in a relatively uniform density distribution at a long-range scale that is similar to HS or charged HS systems. Here, we discuss the phase diagrams before discussing the structures and dynamics at different phase regions.

Equilibrium phase diagrams
An SALR system has a very rich phase diagram. Its equilibrium phase diagram for type-I and type-II SALR systems is mostly studied by computer simulations and lysozyme samples in low-salinity solutions. There are only a few works on the type-III SALR systems by theories and computer simulations. Thus, we focus on the type-I and type-II systems but briefly discuss the type-III systems at the end of this section.

The phase diagram of an SALR system is intrinsically linked to the phase diagram of systems with only a short-range attraction. Based on the extended law of corresponding state proposed by Noro and Frenkel, if the range of the attraction is small enough, the equilibrium phase diagram of all systems with a short-range attraction can be converted to a master phase diagram if the effective temperature is expressed with the corresponding Baxter's sticky parameter (or normalized second virial coefficient) [43]. Thus, we start with the classical phase diagram of SHS systems, whose schematic phase diagram is shown in Figure 1(a). At low concentration below the percolation transition, the cluster distribution has a continuous decay without any peak (no clusters with an optimal size). Such a system is defined as the dispersed fluid state [13]. Increasing the concentration causes the formation of percolated clusters to enter the random percolated state [13]. When cooling the temperature, a system enters the two-phase region.

Figure 1
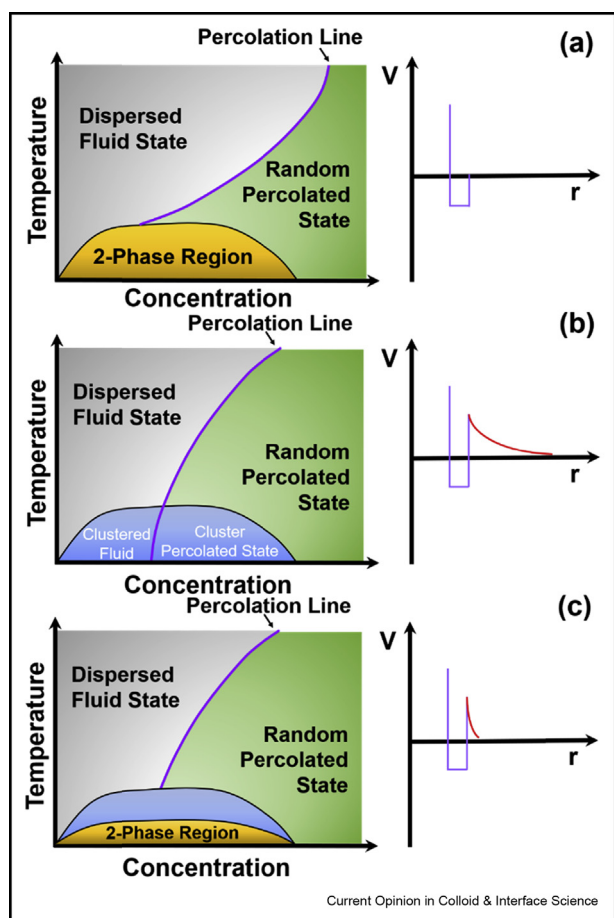
Schematic phase diagrams of **(a)** systems with a short-range attraction, **(b)** systems with a type-II SALR interaction, and **(c)** systems with a type-I SALR interaction. High temperature means a weak attraction. And low temperature means a strong attraction. SALR, short-range attraction and long-range repulsion.

When introducing a long-range repulsion to a system with a short-range attraction, computer simulations show that the cluster size distribution of an SALR system can show a local peak [13,23,49,58]. This indicates there is a formation of clusters with an optimal size that is unique to some SALR systems. Godfrin et al. defined a clustered fluid state if there is a cluster formation with an optimal size. By studying many type-II and a couple of type-I SALR systems, Godfin et al. [13] found that in the one-phase region without any macroscopic phase separation, there can be four different liquid states: dispersed fluid state, clustered fluid state, random percolated state, and cluster percolated state. The schematic picture is shown in Figure 1(b). Note that the existence of the long-range repulsion shifts the percolation line [36]. Interestingly, for the systems they examined, the boundary between the dispersed fluid and clustered fluid states approximately coincides with the binodal transition line of the reference attractive system shown in Figure 1(a). The reference attractive system is defined as the system with the interaction containing only the attractive portion of the total SALR interaction, which is discussed in detail in Ref. [13]. And the boundary between the random percolated and cluster percolated states can be also approximated with the same binodal line of its reference attractive system. Thus, the details of the shape and range of the attraction do not alter the state diagram in Figure 1(b). Hence, a generalized state diagram is proposed to generalize the extended law of corresponding state for systems with a short-range attraction to SALR systems. With the generalized phase diagram proposed by Godfrin et al., the calculation of the transition boundary for an SALR system between the dispersed fluid state and clustered fluid state becomes simple as we only need to estimate the Baxter's sticky parameter using only the attractive portion of an SALR interaction. The same is true to calculate the boundary between a random percolated state and the cluster percolated state.

Except a few cases with the type-I potential parameters, the SALR systems discussed by Godfrin et al. in Ref. [13] are mostly type-II SALR systems where the range of repulsion is comparable to the size of a particle. They briefly discussed that if the range of repulsion becomes smaller, the clustered fluid state may disappear, that is, the repulsion range may not long range enough to maintain clusters with a regular size. There has been no systematic study of the state diagram yet for a wide range of the type-I SALR systems. All four liquid states shown in Figure 1(b) are in the one-phase region. But as shown in Figure 1(c), when the range of the repulsion becomes smaller and smaller, it is reasonable to speculate that there should be a two-phase region of the SALR system as shown in Figure 1(c). This two-phase region should be at lower temperature than that of the binodal line of the reference attractive system. It is expected that the dispersed fluid state and random percolated state boundary above the binodal line of the reference attractive system should be qualitatively similar, even though the structures of liquid states may be different. And the clustered fluid state region and cluster percolated state region should become narrower and eventually may disappear. It is, thus, very interesting to study the structures and dynamics for the systems sandwiched by these two binodal lines: one is the binodal line of the reference attractive system and another one is the binodal line of the SALR system. When the range of the repulsion becomes infinitesimally small, the two-phase region should coincide with that of the reference attractive system. Certainly, more future works are needed to systematically study the phase diagram of the type-I SALR system. In addition, varying the potential parameters continuously can shift the phase diagram from Figure 1(b) to Figure 1(c). It would

be interesting to evaluate the potential parameters at the transition boundary of the phase diagram change, which may or may not coincide with the empirical definition used here to classify different types of SALR colloidal systems.

Experimentally, using lysozyme samples at low-salinity solutions, the state diagram of lysozymes is studied systematically at a wide range of concentrations and temperatures [32]. Based on the interaction potential obtained from the experiments, these lysozyme samples are almost all type-I SALR systems. They are either in the dispersed fluid state or in the random percolated state [32]. Thus, even though there are clusters formed in concentrated lysozyme solutions, there is no optimal cluster size as there is no peak in their cluster size distribution. The temperature dependence of the structure and dynamics are quite different for a sample in the dispersed fluid region or in random percolated region [14,32].

When the range of the attraction becomes much longer than 20% of particle diameter, systems become type-III SALR systems [46,55,59,60]. Archer et al. [46,47,55] studied a type-III SALR system and discovered different liquid−vapor transitions: one is transition from the vapor to a liquid of spherical clusters and another one is the transition to liquids with spherical voids. The equilibrium phase diagram has been also determined. However, there are no experimental systems yet to verify the theoretical predictions in bulk solutions.

Nonequilibrium phase diagrams

Nonequilibrium phase diagrams, for example, gelation and glass transitions, of SALR systems have also been studied. Wu et al. [54] applied the mode coupling theory (MCT) by using the analytical structure factor of two Yukawa potential as inputs to predict the kinetic phase diagram of a type-II SALR system [34]. To address the issue of the large heterogeneity density distribution in SALR systems, cluster MCT approach has been proposed to understand the gelation transition [61]. Using the computer simulation for a type-II SALR system, Sciortino et al. [15] proposed that gelation transitions at low concentrations can be introduced by a glass transition driven by the repulsive interaction between clusters. Even though these theoretical works are useful qualitatively, most experimental systems are still type-I SALR systems. Hence, it is difficult to have a direct quantitative comparison between simulations/theories and experimental results similar to what have been achieved in HS or SHS systems.

Campbell et al. [16] studied the gelation transitions in charged PMMA particles in cycloheptyl bromide and cis-decalin (type-I SALR system). The short-range attraction is the depletion attraction introduced by adding polystyrene polymers. The attraction range and strength can be controlled by the size and concentration of polystyrene polymers. Cluster formation is observed at low particle concentrations. By increasing the concentrations, clusters can percolate to form gels. Gelation transitions happen at the volume fraction ϕ, larger than 0.1 [16].

Klix et al. studied the kinetic phase diagram of charged PMMA particles with the depletion attraction too [17]. The repulsion range estimated at low concentrations is about the size of the particle diameter. Therefore, at low concentrations, this system is at the border line of the type-I and type-II SALR systems. The interaction potential parameters at higher concentrations were not discussed in the article. But it is possible that when the concentration increases, it is likely that this system becomes mostly the type-I SALR system. Figure 2(a) shows the phase diagram of their samples. They have observed Wigner glassy state, cluster glassy state, and gel state. The gel state is a structural arrested state. It is still not clear if Wigner glassy and cluster glassy states are true nonergodic states as they could not measure the mean square displacements long enough to observe a plateau. Note that the volume fraction of the gel state is also larger than 0.1 similar to that is observed by Campbell et al. [16] It is interesting to note that the percolation transition also happens between 0.1 and 0.15 volume fraction for many SALR systems when the attraction is very strong [36]. Therefore, the gelation transition for these experimental systems is likely driven by the percolation [17]. Thus, the physics mechanisms of the gelation transition in these SALR systems are intrinsically different from those SHS systems with the depletion attraction [62] but qualitatively agree with that of other SHS systems with different types of attractions [39,44], such as systems with bridging attractions [39].

Lysozyme samples in low-salinity solutions (type-I SALR systems) have also been studied in a wide range of concentration [14,32]. The true structural arrested transition has not been experimentally observed in low-salinity lysozyme samples. As shown in Figure 2(b), at relative dilute conditions, all lysozyme samples (symbols) are in the dispersed fluid states [32]. By increasing the concentration, they enter the random percolated state. But the mean square displacements of samples are still very large indicating mobile particles. By further increasing the concentrations, the normalized mean square displacement of lysozymes becomes comparable to that of glassy states observed by Klix et al. [14,17,32]. Therefore, these lysozyme samples are proposed to be in a locally glassy state. Figure 2(b) shows that the locally glassy state is deep inside the random percolated state. Note that for all samples studied in Refs. [14, 32], they all show Newtonian behavior as a function of shear rate even for the samples in locally glassy states. The shear thinning region happens only at the shear rate above

Figure 2
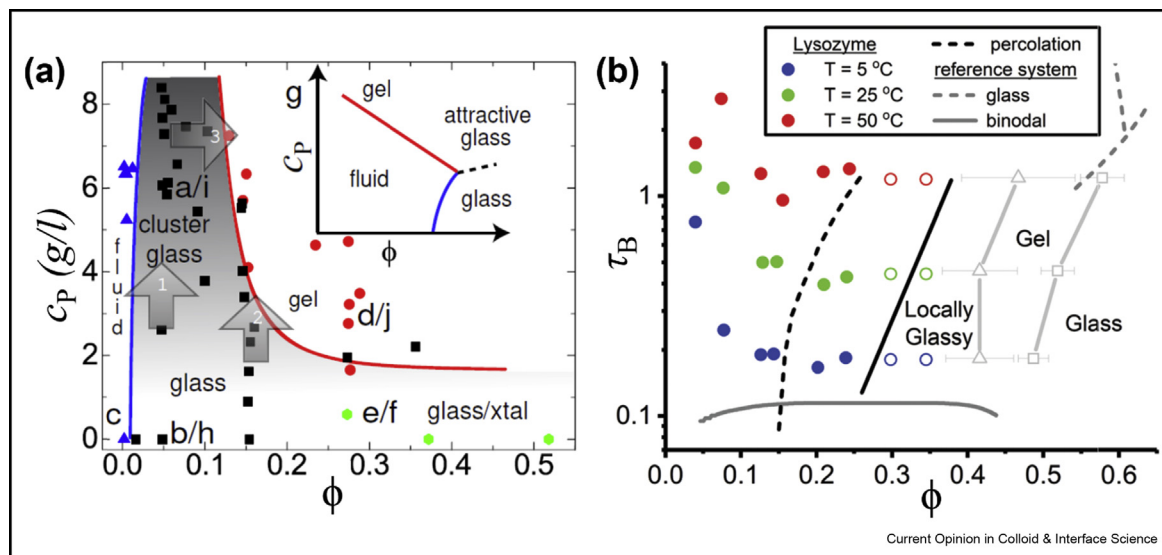
Phase diagram of **(a)** glass and gelation transitions of a PMMA particle with both an SALR interaction; (Reprinted with permission from Ref. [17] Copyright (2010) by the American Physical Society. https://doi.org/10.1103/PhysRevLett.104.165702.) and **(b)** lysozyme samples at low-salty solutions [32]. (Reproduced by permission of The Royal Society of Chemistry).

about 10^4 s^{-1} [63]. These locally glass states are driven by the formation of the IRO in lysozyme samples [14].

Even though an experimental structural arrest transition is not directly observed in lysozyme samples, the gel state is estimated by fitting the viscosity data with a power-law dependence [32]. The volume fraction at which the diffusion coefficients reach zero is determined, which is identified as a glass transition line. Both the estimated gelation transition and glass transition lines are shown in Figure 2(b). Hence, by increasing the lysozyme concentration, it can sequentially experience the following states: dispersed fluid state, random percolated state, locally glassy state, gel state, and glass state [32]. It is noted that the gelation transition line was also estimated in a lysozyme sample with HEPES (*4-(2-hydroxyethyl)-1-piperazineethanesulfonic acid*) buffer at pH = 7.8 [64]. And its gelation transition volume fraction at room temperature is smaller than that shown in Figure 2(b), which may be due to different potentials caused by the different buffer conditions used to prepare samples.

It is noted that the cluster glassy and Wigner glassy states for PMMA systems are observed at the volume fractions much smaller than the percolation transition. And the gelation transition for PMMA particles happens around 0.1 volume fraction very close to the percolation transition [17]. However, for lysozyme samples at low-salinity conditions, no glassy or gel states are observed before and around the percolation transitions. Even the locally glassy states are deep inside the random

percolated regions. It is still not clear what cause these two types of experimental systems to behave differently. Certainly, the potential parameters are different in these two experimental systems. And the mechanisms of the attraction for PMMA particle solutions are different from that between lysozyme proteins. And the diameter of a lysozyme is about 3.4 nm that is about 500 times smaller than some PMMA particles [12]. The large size difference between these two experimental systems can play a role too. Future works are needed to illustrate the relationship between systems with dramatically different particle sizes.

Structure properties of SALR systems

The competition of the short-range attraction and long-range repulsion introduces an additional ordering at the length scale much larger than the particle diameter. This intermediate range order (IRO can be readily observed in both experimental and simulation results by obtaining the interparticle structure factor.

IRO in SALR systems

The IRO is always associated with the appearance of a special peak in the interparticle structure factor, $S(Q)$, whose peak position is much smaller than the position of the first diffraction peak between monomers. Here, Q is the scattering wave vector. This low-Q peak, which is termed as an IRO peak, is the hallmark feature of many SALR systems [11,12,15,34,58]. It was initially attributed to the correlation between clusters with an optimal size in solutions by studying concentrated lysozyme

solutions [11]. However, it was later found the relationship between this low-Q peak and the particle structure is much more complicated [22,48,66]. By combining the diffusions measured by the neutron spin echo (NSE) and interparticle structure factor, $S(Q)$, measured by small angle neutron scattering, Liu et al. conclusively demonstrated that this low-Q peak is not necessarily related with the clusters with optimal sizes in solutions and should be more appropriately termed as an IRO peak [12].

Figure 3(a) shows one typical example of IRO peaks calculated with the integral equation theory for a type-I SALR system [12]. A schematic SALR interaction is shown in Figure 3(b). Figure 3(c)−(f) shows the images of a few systems with IRO structures. Figure 3(c) is the reconstructed experimental image of PMMA particles in an organic solvent (type-I SALR system) [16]. Figure 3(d) is the snapshot of type-II SALR systems using computer simulations [13]. Figure 3(e) is the snapshot of a type-III SALR system at fairly high particle concentrations [47]. And Figure 3(f) is the simulation picture of quantum dots at air−water interface driven by a SALR interaction [65]. There are many other experimental systems with IRO structures

[12,31,51,67,68]. Note that the prominence of the IRO peak depends on the attraction strength and range of the attraction and repulsion. When the attraction becomes weaker and weaker, the height of the IRO peak becomes smaller and smaller. And eventually, $S(Q)$ becomes similar to that of systems with pure repulsive interactions.

Experimentally, it has been shown that the position of the IRO peak in some lysozyme protein solutions is independent of protein concentrations [11,69]. Based on the calculation of the integral equation theory, it has been demonstrated that if the interaction potential parameters are not changed, the position of the IRO peak can remain the same for a very wide range of particle concentration [12,34]. This can be seen also for the $S(Q)$ shown in Figure 3(a).

Relationship between the IRO peak and the cluster formation

Because the appearance of the IRO peak can be associated with many different types of structures, many efforts have been devoted to understanding the relationship between the IRO peak and the cluster formation at low particle concentrations. However, as pointed

Figure 3
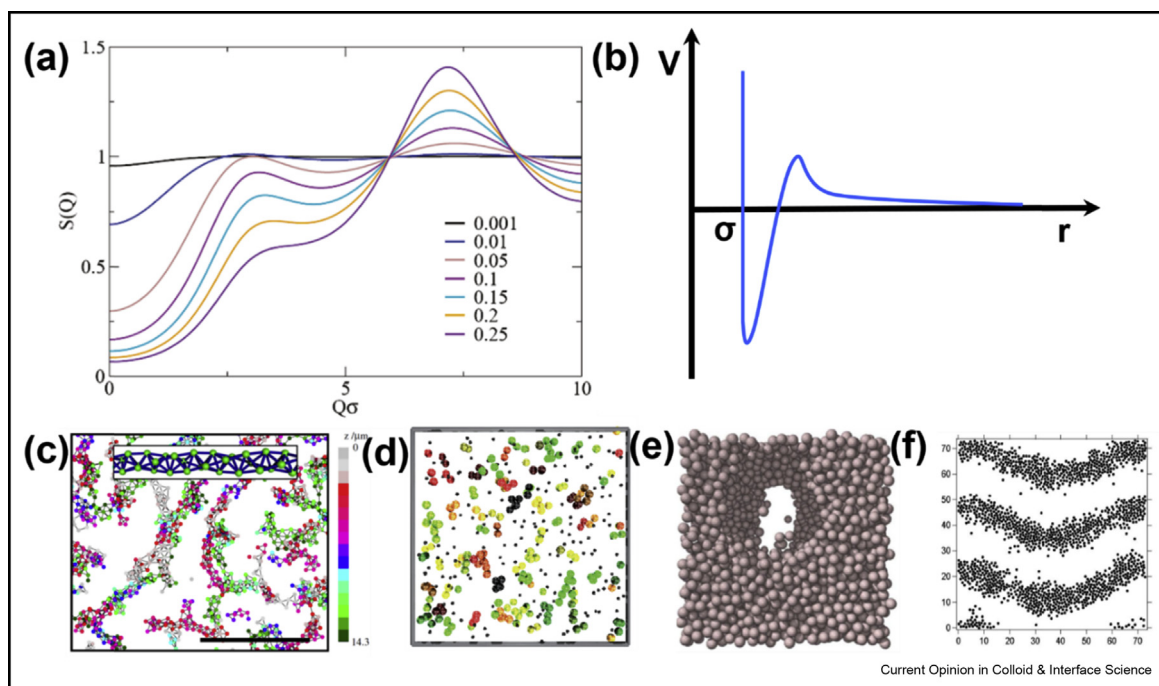
Typical IRO peak and structures of SALR systems are shown here. **(a)** Calculated $S(Q)$ of an SALR interaction using the integral equation theory; Reprinted with permission from Ref. [10]. Copyright (2011) American Chemical Society. **(b)** A schematic plot of an SALR interaction; **(c)** the reconstructed experimental image of the particle arrangement in a gel phase (type-I SALR system); Reprinted with permission from Ref. [16] Copyright (2005) by the American Physical Society. https://doi.org/10.1103/PhysRevLett.94.208301. **(d)** A snapshot of the particles by a computer simulation (type-II SALR system) [13]; (Reproduced by permission of The Royal Society of Chemistry). **(e)** A computer simulation picture of a type-III SALR system; (Reprinted with permission from Ref. [47]. Copyright (2007) by the American Physical Society. https://doi.org/10.1103/PhysRevE.76.031501.) (f) A computer simulation image of an SALR system at the air−water interface. (Reprinted with permission from Ref. [65] Copyright (1999) by the American Physical Society. https://doi.org/10.1103/PhysRevE.59.R6255.) SALR, short-range attraction and long-range repulsion.

out recently, cluster formation is actually a complicated concept [12,22,32]. Therefore, it is useful to briefly discuss the definition of cluster formation on the basis of computer simulations and experimental observations. Some details can be found in Ref. [32].

Many works by computer simulations consider two particles to be bound together if their distance is smaller than a certain cutoff distance [13,15]. Clusters determined in this way is recently termed as geometrically connected clusters (GCCs) to distinguish them from the clusters observed by some experimental techniques [32]. Even though the definition of GCC is very useful, it has some intrinsic problems. Owing to the density fluctuation caused by Brownian motions in solutions, particles without attractions can form many GCCs as some particles can move close to each other in solutions that are not driven by any attraction. So, even HS systems can have many GCCs. In addition, almost no experiment techniques can directly determine GCCs reliably in solutions, even though confocal microscope might have a chance to directly image the particle arrangements if particles are big and their motions are slow enough. To make things more complicated, not all clusters formed in a system are the same. To distinguish different types of clusters, it has been proposed that based on the dynamic features of clusters, they can be approximately classified as transient clusters, dynamic clusters, and permanent clusters [12,22]. However, the GCC has no built-in information of the dynamics. In fact, in many cases, the transient clusters may dominate the GCCs [32]. Therefore, we need to be cautions with comparing the cluster formation results from computer simulations with those from experiments.

Nevertheless, most computer simulations use the GCC definition to find the relationship between the IRO peak and the cluster formation. In particular, the focus has been on how to determine a cluster phase with an optimal size, which only happens if a sample is in clustered fluid states as shown in Figure 1(b). But in many experiments, the interaction potential is not available. Therefore, it is desirable to determine the clustered fluid phase directly from $S(Q)$ that can be experimentally measured by small angle neutron scattering or small angle X-ray scattering (SAXS).

By studying many type-II SALR systems, Godfrin et al. [13] find that when the peak height of the IRO peak is 2.7 or higher, a system is likely in the clustered fluid state. An alternative criterion based on the peak width of the IRO peak has also been later proposed by Jadrich et al. [23]. By studying type-II SALR systems, they show that the peak width is related with the thermal correlation length. If the thermal correlation length is equal or larger than the range of the repulsion, a system should be in the clustered fluid state. By comparing the criteria based on the height and width of the IRO peak,

a combined criterion is then proposed that an SALR system is most likely in a clustered fluid state if the following two conditions can be simultaneously satisfied: (1) the height of the IRO peak is about 2.7 or larger and (2) the thermal correlation length normalized by the particle diameter is between 2 and 3 [50]. Note that it has been shown that when the repulsion range becomes small, that is, for many type-I SALR systems, the prediction based on the previous criterion becomes less and less satisfactory [50]. In general, the aforementioned criteria work well for the type-II SALR systems but should be considered as necessary conditions for a system in a clustered fluid state for the type-I SALR systems. Therefore, if the peak height of the IRO peak is less than 2.7, a system can only be in a dispersed fluid state or a random percolated state.

Interestingly, for most lysozyme experiments, the height of the IRO peak is always smaller than 2.7, which indicates that most experimentally studied lysozyme samples in low-salinity solutions are not in clustered fluid states. This shows that the clusters formed in lysozyme solutions has no optimal sizes. It is noted that there is also a proposal to observe the cluster formation by examining the value of the pair distribution function at the contact point [70].

Cluster morphology
Cluster formation is observed in all SALR systems. Here, we focus on discussing the morphology of clusters in different type of SALR systems, no matter if a system is in a clustered fluid state or not.

The cluster morphology is strongly affected by the interaction parameters. Experimentally, the cluster morphology has been mostly studied with PMMA particles in organic solvent. Campbell et al. studied charged PMMA spheres with a long-range repulsion with $Z \approx 1.6$ (type-I SALR system) [16]. They observed the formation of elongated rod-like aggregates (Bernal spirals shown in Figure 3(c)), which is later confirmed by a computer simulation too [71]. Zhang et al. studied similar PMMA systems with $Z \approx 0.5$ (type-II SALR system) [45,72]. They found that when the attraction strength is relatively small, the formed clusters are compact microcrystalline clusters that are thermodynamically stable. However, when the strength of the short-range attraction is very strong, quasi-linear clusters can form and are nonequilibrium clusters. The route to gels is, thus, affected by the type of clusters driven by different attraction strength [45].

It is important to point out that for PMMA particles in solutions, the interaction parameters are usually determined or estimated at the relatively low concentrations [16,17]. However, the possible change of the interaction parameter as a function of concentration has not been

reported in the works mentioned previously. So, it is possible that changing the particle concentrations can shift the type-II SALR system to type-I SALR system. Future experiments are needed to investigate this.

The morphology of clusters at equilibrium conditions has been extensively studied by computer simulations. For small particle concentrations, many works show that the cluster morphology is not sensitive to the particle concentration [71]. When the range of the repulsion is only a fraction of the particle diameter (type-I SALR system), the isolated small clusters tend to have elongated shape, such as Bernal spirals [49,71]. However, when the repulsion range is comparable or larger than the particle diameter (type-II SALR systems), clusters tend to be more compact and spherical-like [49]. In this situation, it has been argued that it is possible to define the cluster–cluster interaction between these compact clusters for type-II SALR systems [15,49]. Not surprisingly, introducing the size polydispersity can affect the packing of the clusters and frustrate the formation of microcrystalline clusters [50]. Fractal dimension, d_f, of clusters in SALR systems is different for small and larger clusters. d_f of large clusters (the number of particles in a cluster is larger than 10) is sensitive to both the attraction and repulsion [71]. For many SALR systems, d_f of large clusters tends to be small, such as 1.3 to 1.55 [49,71]. However, note that a different simulation seems to indicate that $d_f \approx 3$ [50].

The local packing volume fraction was experimentally found for both PMMA particles and lysozyme solutions to be around 0.4 inside clusters in type-I SALR systems [16,32]. Computer simulations for many type-II SALR systems and a few type-I SALR systems also confirm the local volume fraction inside clusters to be about 0.4 [50]. In the clustered fluid state, the average coordination number of particles inside the clusters is found to be around 2.4 [13], which happens to be the average coordination number of SHS at the gelation transition due to the rigidity percolation [13].

Dynamic properties of SALR systems
Any structure change of a system should be associated with the corresponding dynamic change. The emergence of the IRO means that additional dynamic features should appear in a SALR system. For colloidal systems in solutions, the characteristic time, τ_D, for a system is usually defined as $\tau_D = \frac{\left(\frac{\sigma}{2}\right)^2}{D_0}$, where D_0 is the free diffusion coefficient. For the dynamics associated with the time scale much shorter than τ_D and larger than the momentum relaxation time, it has been called short-time dynamic behavior. And for the time scale much longer than τ_D, it is considered to be at the long-time limit [73]. For SALR systems, the short-time diffusion, $D_{c,s}$, and long time diffusion coefficients, $D_{c,L}$, have

been the interests of studies. The subscript, 'c', indicates the collective diffusion coefficient. $D_{c,s}(Q)$ depends on Q and can be measured with scattering techniques. At relatively low concentrations, the difference between $D_{c,s}$ and $D_{c,L}$ can be very small. But it can be significantly different at high concentrations.

Short-time behavior
The short-time dynamic behavior of SALR systems has been widely studied to understand the cluster formation in concentrated solutions. Based on the life time of clusters, clusters in solutions have been classified as three different types of clusters: transient clusters, dynamic clusters, and permanent clusters. If the lifetime of a cluster is smaller than τ_D, a cluster is a transient cluster. If the lifetime is finite and larger than τ_D, a cluster is a dynamic cluster. For a permanent cluster, its lifetime is expected to be larger than most experiment time needed for measuring the macroscopic properties. Details about the different types of clusters can be found in Refs. [12, 22]. The dynamic cluster formation has been studied for solutions with lysozyme [12,22], monoclonal antibody [25,28], villin headpiece proteins [74], Keggin-type heteropolyanions [67], insulin [75], bovine serum album, and γ-globulin proteins [76].

To study the dynamic cluster formation in lysozyme solutions (type-I SALR systems), the asymptotic value of $D_{c,s}(Q)$ has been measured up to about 20% volume fraction, whose high Q value is the self-diffusion coefficient, $D_{s,s}$ [22]. $D_{s,s}/D_0$ is shown to decay with a linear relation as a function of the volume fraction. By fitting it with a linear equation, $\frac{D_{s,s}}{D_0} = 1 - \lambda\phi$, λ is found to be approximately 3.9 [22]. Here, ϕ is the volume fraction. In comparision, λ is 1.8 for HS systems. For charged HS systems, λ is even smaller. Thus, λ for the lysozyme protein solution at low-salinity solutions is much larger than that of HS and charged HS systems.

The significant smaller value of $D_{s,s}$ as a function of concentration compared with other systems, such as HS systems, is attributed to the formation of dynamic clusters in lysozyme solutions [12,22]. This is not surprising as strongly bounded clusters should have slower motions than nonbounded protein monomers. Thus, by studying $D_{s,s}$, strongly bounded small clusters can be probed. Using this method, the formation of dynamic clusters of concentrated lysozyme solutions in low-salinity conditions is found [22]. This method has been extended and applied to monoclonal antibody solutions, in which the interaction potential in some cases can be qualitatively approximated with an isotropic SALR interaction [25,28].

The advantage of using $D_{s,s}$ to investigate dynamic clusters is that $D_{s,s}$ is not strongly affected by caging. However, the challenge for this method is how to estimate the contribution of the hydrodynamic effect of

formed clusters on $D_{s,s}$. An approximate method using the HS model has been used to roughly correct the hydrodynamic effect of clusters to approximately evaluate the hydrodynamic radius of dynamic clusters in lysozyme solutions [22].

The attraction strength between lysozyme proteins in solution sensitively depends on the temperature. By changing the temperature from 50 °C to 4 °C, the overall short-range attraction can change from negligibly small to strongly attractive on the basis of the estimated sticky parameters [32]. As a result, there can be no visible IRO peak in $S(Q)$ for lysozyme proteins at 50 °C, whereas $S(Q)$ of the sample can have a very strong IRO peak at 4 °C [14]. The temperature studies for lysozyme samples in the dispersed fluid region show that $D_{s,s}/D_0$ does not change much in a wide temperature range [32,77]. Thus, it is concluded that clusters formed in the dispersed fluid regions are mostly transient clusters. Note that simulation works show that many GCCs can form at similar concentrations for SALR systems. Thus, the observed GCCs in the dispersed fluid regions in SALR systems are believed to be mostly transient clusters [32].

However, once a system is in the random percolated state, results from lysozyme samples (type-I SALR system) show that $D_{s,s}/D_0$ becomes very sensitive to the short-range attraction strength. Therefore, dynamic clusters begin to dominate the systems.

For protein solutions, τ_D is very small owing to the small sizes of proteins. For example, $\tau_D \approx 25$ ns for lysozyme in heavy water at room temperature. And for larger proteins, such as monoclonal antibody, τ_D is approximately around a few hundred nanoseconds. To probe the dynamics at the short-time limit and access the Q range comparable to a protein size, NSE has been found to be a very useful tool to obtain the short-time diffusion coefficient, $D_{c,s}(Q)$. Also, NSE can probe $D_{s,s}(Q)$ by measuring relative high Q values without labeling a protein. The signal of macromolecule systems measured by NSE is discussed in Ref. [78]. However, because NSE can only measure the correlation time less than one microsecond, it is only sensitive to strongly bounded small clusters. When dynamic clusters grow too big at high concentrations, NSE is only sensitive to local motions of monomers inside a large cluster.

For micrometer-sized large colloidal particles, τ_D can be as large as a few seconds. However, there are currently no systematical studies of $D_{s,s}$ as a function of concentration in liquid states for these large model particles. Most recent studies of large PMMA particles have been focused on gel or glass states rather than the liquid states. It would be interesting to study $D_{s,s}$ in model spherical particles and compare the results with that from protein solutions in future.

Applying liquid theories, Riest et al. have systematically calculated $D_{c,s}(Q)$, the short-time hydrodynamic function ($H(Q)$), and the high-frequency viscosity ($\eta_\infty(\phi)$) in type-I and type-II SALR systems [56]. Interestingly, an IRO peak is observed in $H(Q)$. The IRO peak is also observed in the experimentally obtained $H(Q)$ [79]. The comparison of $H(Q)$ from the experiment and the theoretical prediction shows that there is a quantitative agreement at relatively low concentration in the dispersed fluid region [79]. It is important to point out that this comparison is made without any adjustable parameters. However, when the lysozyme protein concentration increases, the deviation of the theoretical values from the experimental results becomes larger [79]. Theoretical calculation also shows that $D_{c,s}(Q)$ shows very small variations once Q is larger than the IRO peak position, which is consistent with the experimental observations [22,77]. This is very useful for NSE experiments as it does not need to measure signals at very high Q values to obtain $D_{s,s}$, which makes measurements faster.

Viscosity and long-time behavior

Viscosity is an important macroscopic property of colloidal systems. For protein solutions, the viscosity is linked to the long-time behavior of protein motions. Note that understanding protein viscosity in concentrated protein solutions has been a critical problem for the pharmaceutical industry as concentrated therapeutic protein solutions are desirable for the subcutaneous injection methods in clinic applications [1]. Viscosity is one of key parameters when the industry formulates the final protein products. Interested readers can read a recent review article about the study of the protein solution viscosity [1]. As many proteins have SALR interactions in low-salinity solutions, the study of the viscosity of SALR systems can help shed light onto the viscosity control of industrial products in addition to the fundamental interests.

The zero shear viscosity of lysozyme samples (type-I SALR system) has been measured at different conditions [14,64]. A recent study showed that the temperature dependence of the relative viscosity of lysozyme samples depends on the concentration [14]. At relative low concentration, when the samples are in the dispersed fluid state, the relative viscosity is not sensitive to the temperature. At the random percolated state, the viscosity is very sensitive to the temperature. In fact, for one very concentrated lysozyme sample, the viscosity can increase by more than 100 times when the temperature decreases from 50 °C to 4 °C. This change is due to the increase of the attraction between lysozymes by decreasing temperature (note that the physical origin of the attraction between many proteins remains a research topic as many factors contribute to its attraction, such as hydrophobic patches, charge distribution, and coion/counterion effects [9,29,41].) MCT

theory has been applied to explain the viscosity change of SALR systems [56,79]. And interestingly, the theoretical predictions agree reasonably well with the experimental data for the concentration up to about 20% volume fraction [79]. For large colloidal model particles, we are not aware of the systematic study of the viscosity behavior in SALR systems.

By applying the generalized Stoke−Einstein relation, the long-time self-diffusion coefficient, $D_{s,L}$, is estimated and used to calculate the mean square displacement at long time [14]. Interestingly, it is shown that in lysozyme samples (type-I SALR system), the short-time and long-time behavior agrees with each other at the particle volume fraction up to about 15%. Thus, $D_{s,L}$ and $D_{s,s}$ are the same. In fact, an earlier work using nuclear magnetic resonance to measure $D_{s,L}$ shows that within the experimental error bars, $D_{s,L}$ is the same as $D_{s,s}$ for the volume fraction up to about 20% at room temperature [12]. However, at higher lysozyme concentrations, the estimated $D_{s,L}$ becomes smaller than $D_{s,s}$. At about 37% volume fraction and low temperature (4 °C), $D_{s,L}$ is even smaller than 10% of $D_{s,s}$ [32]. Note that for HS systems, if $D_{s,L}/D_{s,s} < 10\%$, a system begins to form colloidal crystals. And this is called the Löwen criterion. Thus, it seems that the Löwen criterion can be violated in SALR systems. It is noted that the cluster formation in lysozyme samples has also been studied using NRM by observing the long-time behavior [80].

Two-dimensional SALR systems

We have so far focused on the review of the bulk SALR systems. SALR systems in two-dimension also show interesting behavior, which are important for the understanding of many arrangement of particles at the interface, such as air−water interface or in-film arrangements in cell membranes. Some works on two-dimensional SALR systems show that particles can self-assemble into interesting patterns [57,81,82]. The quantum dots at the air−water interface show interesting spontaneously formed patterns, such as circular clusters and stripe-like arrays, which can be explained by the competition of an SALR [65,83]. The range of the attraction in studies on two-dimensional systems tends to be longer than that of the type-I SALR system [57,81,83]. The study of two-dimensional SALR systems with a short-range attraction demonstrates that for two-dimension system with the type-II interaction, gelation may happen due to the structure arrested transition of microphase separations [84].

Summaries and perspectives

The colloidal science community has seen the increased research interests in studying colloidal systems with both a short-range attraction and long-range repulsion in the past decade, which are the natural extension of well-studied HS, SHS, and charge HS systems. The competition of the attraction and repulsion introduces different kinds of IRO structures, and hence provides a different way to control the solution structures and self-assembly of colloidal particles that can potentially become new routes to make interesting materials. Since the protein−protein interaction of many protein systems has both a short-range attraction and long-range repulsion, the study of SALR systems is expected to greatly benefit the protein community to understand concentrated protein solutions, which are commonly encountered in both industrial applications and many biological conditions.

Much progress has already been made in the past decade in understanding the structures, dynamics, and the phase diagrams of SALR systems. However, owing to the large parameter spaces available for SALR systems, we are far from full understanding of SALR systems. It seems that most computer simulation and theoretical works have been focused on type-II and type-III SALR systems. However, majority of experimental systems, no matter they are proteins or micrometer-sized model colloidal particles, are mostly type-I SALR systems. Therefore, many future computer simulation and theoretical works are needed to fully understand the type-I SALR systems, while more experimental systems need to be developed for type-II and type-III SALR systems to test the predictions by theories and simulations. In addition, the nonequilibrium phase diagram observed from protein systems and the PMMA colloidal systems show qualitative difference. Future works are needed to reconcile these differences. The study of SALR systems at the interface has received less attention. However, the interesting spontaneous patterns already observed in both experiment and simulation/theory indicate that more future work on both experiment and simulation may lead to exciting discoveries for two-dimensional systems.

Currently, majority of studies on SALR systems have been focused on isotropic effective interactions. However, it has been demonstrated that introducing patchy short-range attraction to HS systems can generate a rich phase behavior. Therefore, it is reasonable to expect that introducing patchy interactions to SALR systems can strongly impact the structure, dynamics, and the phase diagrams compared with SALR systems with isotropic interactions. Because it is very likely that there are patchy attractions and/or charges for many protein systems, applying the patchy interaction to SALR systems may lead us one step closer to fully understand the solution behavior of concentrated protein solutions.

Even though the equilibrium structure and phase diagrams are expected to be similar as long as the effective

potential is identical, systems with the same effective potential but with different physics origins can have different dynamics and nonequilibrium phase diagrams. For example, changing from the depletion attraction to the bridging attraction can significantly shift the gelation transition [39]. It is, thus, interesting to see future works to understand how the different types of origins of attractions, such as interaction introduced by the correlation of counterions, can affect the dynamics and nonequilibrium phase diagrams.

Conflicts of interest statement

Nothing declared.

Acknowledgements

References

1. Zhang ZH, Liu Y: **Recent progresses of understanding the**
* **viscosity of concentrated protein solutions**. *Curr Opin Chem Eng* 2017, **16**:48−55.
This is a short-review article that has discussed the interaction effect on the protein viscosity including proteins systems with SALR interactions.

2. Anderson VJ, Lekkerkerker HNW: **Insights into phase transition kinetics from colloid science**. *Nature* 2002, **416**:811−815.

3. Cheng W, Wang JJ, Jonas U, Fytas G, Stefanou N: **Observation and tuning of hypersonic bandgaps in colloidal crystals**. *Nat Mater* 2006, **5**:830−836.

4. Zaccarelli E: **Colloidal gels: equilibrium and non-equilibrium routes**. *J Phys Condens Matter* 2007, **19**:50.

5. Pusey PN, Vanmegen W: **Phase-behavior of concentrated suspensions of nearly hard colloidal spheres**. *Nature* 1986, **320**:340−342.

6. Pham KN, Puertas AM, Bergenholtz J, Egelhaaf SU, Moussaid A, Pusey PN, Schofield AB, Cates ME, Fuchs M, Poon WCK: **Multiple glassy states in a simple model system**. *Science* 2002, **296**:104−106.

7. Yethiraj A, van Blaaderen A: **A colloidal model system with an interaction tunable from hard sphere to soft and dipolar**. *Nature* 2003, **421**:513−517.

8. Verwey EJW: **Theory of the stability of lyophobic colloids**. *J Phys Colloid Chem* 1947, **51**:631−636.

9. Tardieu A, Le Verge A, Malfois M, Bonnete F, Finet S, Ries-Kautt M, Belloni L: **Proteins in solution: from X-ray scattering intensities to interaction potentials**. *J Cryst Growth* 1999, **196**:193−203.

10. Liu Y: **Colloidal systems with both a short-range attraction and a long-range repulsion**. *Chem Eng Process Tech* 2013, **1**:4.

11. Stradner A, Sedgwick H, Cardinaux F, Poon WCK, Egelhaaf SU,
* Schurtenberger P: **Equilibrium cluster formation in concentrated protein solutions and colloids**. *Nature* 2004, **432**:492−495.
This paper studied lysozyme and PMMA particles in low salinity solutions and demonstrated the appearance of low-Q peak in the structure factor.

12. Liu Y, Porcar L, Chen JH, Chen WR, Falus P, Faraone A,
** Fratini E, Hong KL, Baglioni P: **Lysozyme protein solution with an intermediate range order structure**. *J Phys Chem B* 2011, **115**:7238−7247.
Combining with the NSE and SANS results, the authors demonstrated that the low-Q peak in the structure factor for SALR systems should be termed an IRO peak, and the cluster formation in solutions has a complex relationship with the IRO peak. And the properties of transient cluster, dynamic cluster, and permanent clusters are discussed.

13. Godfrin PD, Valadez-Perez NE, Castaneda-Priego R, Wagner NJ,
** Liu Y: **Generalized phase behavior of cluster formation in colloidal dispersions with competing interactions**. *Soft Matter* 2014, **10**:5061−5071.
Using the computer simulations, the authors studied the one-phase region of SALR systems and found four different liquid states: dispersed fluid state, clustered fluid state, random percolated state, and cluster percolated state. The relationship of these liquid states with that of the reference attractive systems is determined. And the relation between the height of the IRO peak and the liquid state is studied.

14. Godfrin PD, Hudson SD, Hong K, Porcar L, Falus P, Wagner NJ,
** Liu Y: **Short-time glassy dynamics in viscous protein solutions with competing interactions**. *Phys Rev Lett* 2015, **115**:228302.
By using the NSE to obtain the mean square displacement of concentrated lysozyme solutions, locally glassy states are found. It is driven by the formation of the IRO. The viscosity change in a wide range of the temperature is also reported for lysozyme solutions.

15. Sciortino F, Mossa S, Zaccarelli E, Tartaglia P: **Equilibrium**
** **cluster phases and low-density arrested disordered states: the role of short-range attraction and long-range repulsion**. *Phys Rev Lett* 2004, **93**.
Using the computer simulation to study the type II SALR systems, the authors demonstrated that the gelation transition in these SALR systems is driven by the structural arrest transitions of clusters formed by the competition of the short-range attraction and long-range repulsion.

16. Campbell AI, Anderson VJ, van Duijneveldt JS, Bartlett P:
** **Dynamical arrest in attractive colloids: the effect of long-range repulsion**. *Phys Rev Lett* 2005, **94**.
Using charged PMMA particles as model systems (type I SALR system), the authors demonstrated the formation of elongated and ordered clusters (Bernal Spirals) driven by a SALR interaction. And their systems gel due to the cluster growth and association.

17. Klix CL, Royall CP, Tanaka H: **Structural and dynamical fea-**
** **tures of multiple metastable glassy states in a colloidal system with competing interactions**. *Phys Rev Lett* 2010, **104**.
Using charged PMMA particles as model systems, the authors measured the mean square displacements of their samples, from which they identified the non-equilibrium phase diagram and found Wigner glassy state, cluster glassy state, and gel state.

18. Tardieu A, Finet S, Bonnete F: **Structure of the macromolecular solutions that generate crystals**. *J Cryst Growth* 2001, **232**:1−9.

19. Piazza R: **Protein interactions and association: an open challenge for colloid science**. *Curr Opin Colloid Interface Sci* 2004, **8**:515−522.

20. George A, Wilson WW: **Predicting protein crystallization from a dilute-solution property**. *Acta Crystallogr Sect D Biol Crystallogr* 1994, **50**:361−365.

21. Abramo MC, Caccamo C, Costa D, Pellicane G, Ruberto R, Wanderlingh U: **Effective interactions in lysozyme aqueous solutions: a small-angle neutron scattering and computer simulation study**. *J Chem Phys* 2012, **136**.

22. Porcar L, Falus P, Chen WR, Faraone A, Fratini E, Hong KL,
** Baglioni P, Liu Y: **Formation of the dynamic clusters in concentrated lysozyme protein solutions**. *J Phys Chem Lett* 2010, **1**:126−129.
The authors classified the clusters into transient clusters, dynamic clusters, and permanent clusters based on the dynamic properties of clusters. Using the NSE to measure the short-time diffusion coefficients of concentrated lysozyme samples, they observed dynamic clusters in concentrated lysozyme solutions at low salinity conditions.

23. Jadrich RB, Bollinger JA, Johnston KP, Truskett TM: **Origin and**
* **detection of microstructural clustering in fluids with spatial-range competitive interactions**. *Phys Rev* 2015, **91**.
This paper studies the width of the IRO peak and its relationship with the thermal correlation length. And a criterion is proposed to identify the clustered fluid state using the width of the IRO peak.

24. Groenewold J, Kegel WK: **Anomalously large equilibrium clusters of colloids**. *J Phys Chem B* 2001, **105**:11702−11709.

25. Godfrin PD, Zarraga IE, Zarzar J, Porcar L, Falus P, Wagner NJ, Liu Y: **Effect of hierarchical cluster formation on the viscosity of concentrated monoclonal antibody formulations studied by neutron scattering**. *J Phys Chem B* 2016, **120**:278–291.

26. Yadav S, Shire SJ, Kalonia DS: **Factors affecting the viscosity in high concentration solutions of different monoclonal antibodies**. *J Pharmaceut Sci* 2010, **99**:4812–4829.

27. Mitragotri S, Burke PA, Langer R: **Overcoming the challenges in administering biopharmaceuticals: formulation and delivery strategies**. *Nat Rev Drug Discov* 2014, **13**:655–672.

28. Yearley EJ, Godfrin PD, Perevozchikova T, Zhang HL, Falus P, Porcar L, Nagao M, Curtis JE, Gawande P, Taing R, Zarraga IE, Wagner NJ, Liu Y: **Observation of small cluster formation in concentrated monoclonal antibody solutions and its implications to solution viscosity**. *Biophys J* 2014, **106**:1763–1770.

29. Yearley EJ, Zarraga IE, Shire SJ, Scherer TM, Gokarn Y, Wagner NJ, Liu Y: **Small-angle neutron scattering characterization of monoclonal antibody conformations and interactions at high concentrations**. *Biophys J* 2013, **105**: 720–731.

30. Moaseri E, Bollinger JA, Changalvaie B, Johnson L, Schroer J, Johnston KP, Truskett TM: **Reversible self-assembly of glutathione-coated gold nanoparticle clusters via pH-tunable interactions**. *Langmuir* 2017, **33**:12244–12253.

31. Cabezas CAS, Ong GK, Jadrich RB, Lindquist BA, Agrawal A, Truskett TM, Milliron DJ: **Gelation of plasmonic metal oxide nanocrystals by polymer-induced depletion attractions**. *Proc Natl Acad Sci U S A* 2018, **115**:8925–8930.

32. Godfrin PFPD, Porcar L, Hong K, Hudson SD, Wagner NJ, Liu aY:
* * **Dynamic properties of different liquid states in systems with competing interactions studied with lysozyme solutions**. *Soft Matter* 2018.
Using lysozyme samples at low salt conditions as a model system, the authors obtained the interaction potentials and identified the liquid states of lysozyme samples in the generalized phase diagram. Both the short and long time dynamic properties of SALR systems are studied in the dispersed fluid and random percolated liquid states. Locally glassy states, gel states and glass states are estimated in the generalized phase diagram.

33. Ruzicka B, Zulian L, Zaccarelli E, Angelini R, Sztucki M, Moussaid A, Ruocco G: **Competing interactions in arrested states of colloidal clays**. *Phys Rev Lett* 2010, **104**.

34. Liu Y, Chen WR, Chen SH: **Cluster formation in two-Yukawa fluids**. *J Chem Phys* 2005, **122**.

35. Cardinaux F, Stradner A, Schurtenberger P, Sciortino F, Zaccarelli E: **Modeling equilibrium clusters in lysozyme solutions**. *Epl* 2007, **77**.

36. Valadez-Perez NE, Castaneda-Priego R, Liu Y: **Percolation in colloidal systems with competing interactions: the role of long-range repulsion**. *RSC Adv* 2013, **3**:25110–25119.

37. Crocker JC, Matteo JA, Dinsmore AD, Yodh AG: **Entropic attraction and repulsion in binary colloids probed with a line optical tweezer**. *Phys Rev Lett* 1999, **82**:4352–4355.

38. Chen J, Kline SR, Liu Y: **From the depletion attraction to the bridging attraction: the effect of solvent molecules on the effective colloidal interactions**. *J Chem Phys* 2015, **142**:11.

39. Yuan GC, Luo JH, Han CC, Liu Y: **Gelation transitions of colloidal systems with bridging attractions**. *Phys Rev E* 2016, **94**:6.

40. Linse P, Lobaskin V: **Electrostatic attraction and phase separation in solutions of like-charged colloidal particles**. *Phys Rev Lett* 1999, **83**:4208–4211.

41. Curtis RA, Steinbrecher C, Heinemann A, Blanch HW, Prausnitz JM: **Hydrophobic forces between protein molecules in aqueous solutions of concentrated electrolyte**. *Biophys Chem* 2002, **98**:249–265.

42. Valadez-Perez NE, Liu Y, Castaneda-Priego R: **Reversible aggregation and colloidal cluster morphology: the importance of the extended law of corresponding states**. *Phys Rev Lett* 2018, **120**:6.

43. Noro MG, Frenkel D: **Extended corresponding-states behavior for particles with variable range attractions**. *J Chem Phys* 2000, **113**:2941–2944.

44. Eberle APR, Wagner NJ, Castaneda-Priego R: **Dynamical arrest transition in nanoparticle dispersions with short-range interactions**. *Phys Rev Lett* 2011, **106**:4.

45. Zhang TH, Klok J, Tromp RH, Groenewold J, Kegel WK: **Non-
* * equilibrium cluster states in colloids with competing interactions**. *Soft Matter* 2012, **8**:667–672.
Using charged PMMA particles, it is found that at small attraction strength, clusters with microcrystalline phases are observed. However, when the attraction is strong, they observed elongated non-equilibrium clusters.

46. Archer AJ, Pini D, Evans R, Reatto L: **Model colloidal fluid with
* competing interactions: bulk and interfacial properties**. *J Chem Phys* 2007, **126**.
The authors studied the equilibrium phase diagram of type III SALR systems and studied the impact of the repulsion on the liquid–vapor transition.

47. Archer AJ, Wilding NB: **Phase behavior of a fluid with competing attractive and repulsive interactions**. *Phys Rev E* 2007, **76**.

48. Shukla A, Mylonas E, Di Cola E, Finet S, Timmins P, Narayanan T, Svergun DI: **Absence of equilibrium cluster phase in concentrated lysozyme solutions**. *Proc Natl Acad Sci U S A* 2008, **105**:5075–5080.

49. Toledano JCF, Sciortino F, Zaccarelli E: **Colloidal systems with
* competing interactions: from an arrested repulsive cluster phase to a gel**. *Soft Matter* 2009, **5**:2390–2398.
Using the computer simulation to model type II SALR systems, the structure and dynamic properties of clusters are examined.

50. Bollinger JA, Truskett TM: **Fluids with competing interactions.
* * I. Decoding the structure factor to detect and characterize self-limited clustering**. *J Chem Phys* 2016, **145**.
By studying the wide range of potential parameters (mostly type II SALR systems), the relationship between the properties of IRO peaks and the solution structures is discussed.

51. Ioannidou K, Kanduc M, Li LN, Frenkel D, Dobnikar J, Del Gado E: **The crucial effect of early-stage gelation on the mechanical properties of cement hydrates**. *Nat Commun* 2016, **7**.

52. Das S, Riest J, Winkler RG, Gompper G, Dhont JKG, Nagele G: **Clustering and dynamics of particles in dispersions with competing interactions: theory and simulation**. *Soft Matter* 2018, **14**:92–103.

53. Mossa S, Sciortino F, Tartaglia P, Zaccarelli E: **Ground-state clusters for short-range attractive and long-range repulsive potentials**. *Langmuir* 2004, **20**:10756–10763.

54. Wu JL, Liu Y, Chen WR, Cao JS, Chen SH: **Structural arrest transitions in fluids described by two Yukawa potentials**. *Phys Rev E* 2004, **70**.

55. Archer AJ, Ionescu C, Pini D, Reatto L: **Theory for the phase behaviour of a colloidal fluid with competing interactions**. *J Phys Condens Matter* 2008, **20**.

56. Riest J, Nagele G: **Short-time dynamics in dispersions with
* competing short-range attraction and long-range repulsion**. *Soft Matter* 2015, **11**:9273–9280.
The authors theoretically calculated the short-time properties of a type II SALR system, such as hydrodynamic function, short-time diffusion coefficient, sedimentation coefficient, and high-frequency viscosity. An IRO peak is observed in the hydrodynamic function.

57. Campos LQC, Apolinario SWS, Lowen H: **Structural ordering of trapped colloids with competing interactions**. *Phys Rev E* 2013, **88**.

58. Godfrin PD, Castaneda-Priego R, Liu Y, Wagner NJ: **Intermediate range order and structure in colloidal dispersions with competing interactions**. *J Chem Phys* 2013, **139**.

59. Bomont JM, Costa D, Bretonnet JL: **Tiny changes in local order identify the cluster formation threshold in model fluids with competing interactions**. *Phys Chem Chem Phys* 2017, **19**: 15247–15255.

60. Sweatman MB, Fartaria R, Lue L: **Cluster formation in fluids with competing short-range and long-range interactions**. *J Chem Phys* 2014, **140**.

61. Kroy K, Cates ME, Poon WCK: **Cluster mode-coupling approach to weak gelation in attractive colloids**. *Phys Rev Lett* 2004, **92**.

62. Lu PJ, Zaccarelli E, Ciulla F, Schofield AB, Sciortino F, Weitz DA: **Gelation of particles with short-range attraction**. *Nature* 2008, **453**:499. U4.

63. Dharmaraj VL, Godfrin PD, Liu Y, Hudson SD: **Rheology of clustering protein solutions**. *Biomicrofluidics* 2016, **10**:11.

64. Cardinaux F, Zaccarelli E, Stradner A, Bucciarelli S, Farago B, Egelhaaf SU, Sciortino F, Schurtenberger P: **Cluster-driven dynamical arrest in concentrated lysozyme solutions**. *J Phys Chem B* 2011, **115**:7227–7237.

65. Sear RP, Chung SW, Markovich G, Gelbart WM, Heath JR: **Spontaneous patterning of quantum dots at the air-water interface**. *Phys Rev E* 1999, **59**:R6255–R6258.

66. Shukla A, Mylonas E, Di Cola E, Finet S, Timmins P, Narayanan T, Svergun DI: **Reply to Stradner et al.: equilibrium clusters are absent in concentrated lysozyme solutions**. *Proc Natl Acad Sci U S A* 2008, **105**. E76–E76.

67. Bera MK, Qiao BF, Seifert S, Burton-Pye BP, de la Cruz MO, Antonio MR: **Aggregation of heteropolyanions in aqueous solutions exhibiting short-range attractions and long-range repulsions**. *J Phys Chem C* 2016, **120**:1317–1327.

68. Lonetti B, Fratini E, Chen SH, Baglioni P: **Viscoelastic and small angle neutron scattering studies of concentrated protein solutions**. *Phys Chem Chem Phys* 2004, **6**:1388–1395.

69. Broccio M, Costa D, Liu Y, Chen SH: **The structural properties of a two-Yukawa fluid: simulation and analytical results**. *J Chem Phys* 2006, **124**.

70. Bomont JM, Bretonnet JL, Costa D, Hansen JP: **Communication: thermodynamic signatures of cluster formation in fluids with competing interactions**. *J Chem Phys* 2012, **137**.

71. Sciortino F, Tartaglia P, Zaccarelli E: **One-dimensional cluster
** growth and branching gels in colloidal systems with short-range depletion attraction and screened electrostatic repulsion**. *J Phys Chem B* 2005, **109**:21942–21953.
Using computer simulation to investigate a type I SALR system at a wide range of temperature and volume fraction, the cluster morphology is studied and the formation of elongated Bernal spiral clusters is confirmed.

72. Zhang TH, Groenewold J, Kegel WK: **Observation of a micro-crystalline gel in colloids with competing interactions**. *Phys Chem Chem Phys* 2009, **11**:10827–10830.

73. Nagele G: **On the dynamics and structure of charge-stabilized suspensions**. *Phys Rep Rev Sect Phys Lett* 1996, **272**:216–372.

74. Nawrocki G, Wang PH, Yu I, Sugita Y, Feig M: **Slow-down in diffusion in crowded protein solutions correlates with transient cluster formation**. *J Phys Chem B* 2017, **121**: 11072–11084.

75. Erlkamp M, Grobelny S, Faraone A, Czeslik C, Winter R: **Solvent effects on the dynamics of amyloidogenic insulin revealed by neutron spin echo spectroscopy**. *J Phys Chem B* 2014, **118**: 3310–3316.

76. Balbo J, Mereghetti P, Herten DP, Wade RC: **The shape of protein crowders is a major determinant of protein diffusion**. *Biophys J* 2013, **104**:1576–1584.

77. Falus P, Porcar L, Fratini E, Chen WR, Faraone A, Hong KL, Baglioni P, Liu Y: **Distinguishing the monomer to cluster phase transition in concentrated lysozyme solutions by studying the temperature dependence of the short-time dynamics**. *J Phys Condens Matter* 2012, **24**.

78. Liu Y: **Intermediate scattering function for macromolecules in solutions probed by neutron spin echo**. *Phys Rev E* 2017, **95**: 6.

79. Riest J, Nagele G, Liu Y, Wagner NJ, Godfrin PD: **Short-time
* dynamics of lysozyme solutions with competing short-range attraction and long-range repulsion: experiment and theory**. *J Chem Phys* 2018, **148**.
The theoretical calculated results of hydrodynamic function, short-time diffusion coefficient, and the zero shear viscosity are compared with the experimental results from lysozyme samples.

80. Barhoum S, Yethiraj A: **NMR detection of an equilibrium phase consisting of monomers and clusters in concentrated lysozyme solutions**. *J Phys Chem B* 2010, **114**:17062–17067.

81. Liu YH, Chew LY, Yu MY: **Self-assembly of complex structures in a two-dimensional system with competing interaction forces**. *Phys Rev E* 2008, **78**:10.

82. Chen JX, Mao JW, Thakur S, Xu JR, Liu FY: **Dynamical phase of driven colloidal systems with short-range attraction and long-range repulsion**. *J Chem Phys* 2011, **135**.

83. Sear RP, Gelbart WM: **Microphase separation versus the vapor-liquid transition in systems of spherical particles**. *J Chem Phys* 1999, **110**:4582–4588.

84. Charbonneau P, Reichman DR: **Phase behavior and far-from-equilibrium gelation in charged attractive colloids**. *Phys Rev E* 2007, **75**.